

Time Series Case Based Reasoning for Image Categorisation

Ashraf Elsayed¹, Mohd Hanafi Ahmad Hijazi^{1,5}, Frans Coenen¹,
Marta García-Fiñana², Vanessa Sluming³, and Yalin Zheng⁴

¹ Department of Computer Science, University of Liverpool,
Ashton Building, Ashton Street, Liverpool L69 3BX, UK

² Centre for Medical Statistics and Health Evaluation, University of Liverpool,
Shelley's Cottage, Brownlow Street, Liverpool L69 3GS, UK

³ School of Health Sciences, University of Liverpool,

Thompson Yates Building, The Quadrangle, Brownlow Hill, Liverpool L69 3GB, UK

⁴ Department of Eye and Vision Science, Institute of Ageing and Chronic Disease,
University of Liverpool, UCD Building, Liverpool L69 3GA, UK

⁵ School of Engineering and Information Technology, Universiti Malaysia Sabah,
Locked Bag 2073, 88999 Kota Kinabalu, Sabah, Malaysia
{a.el-sayed,m.ahmad-hijazi,coenen,martaf,slumingv,
yalin.zheng}@liverpool.ac.uk

Abstract. This paper describes an approach to Case Based Reasoning (CBR) for image categorisation. The technique is founded on a time series analysis mechanism whereby images are represented as time series (curves) and compared using time series similarity techniques. There are a number of ways in which images can be represented as time series, this paper explores two. The first considers the entire image whereby the image is represented as a sequence of histograms. The second considers a particular feature (region of interest) contained across an image collection, which can then be represented as a time series. The proposed techniques then use dynamic time warping to compare image curves contained in a case base with that representing a new image example. The focus for the work described is two medical applications: (i) retinal image screening for Age-related Macular Degeneration (AMD) and (ii) the classification of Magnetic Resonance Imaging (MRI) brain scans according to the nature of the corpus callosum, a particular tissue feature that appears in such images. The proposed technique is described in detail together with a full evaluation in terms of the two applications.

Keywords: Case Based Reasoning, Image Analysis, Time Series Analysis, Dynamic Time warping.

1 Introduction

In its traditional form Case Based Reasoning (CBR) is typically directed at tabular data. Current research within the domain of CBR seeks to widen the scope of the technology by, amongst other initiatives, applying it to alternative forms

of data such as images, sound, video, etc. There are two principal issues to be considered when applying CBR to non-standard data. The first is how to best represent the input so as to facilitate CBR. The second is the nature of the similarity checking mechanism to be applied. The two issues are closely related. One potential solution is to translate the input data format into an appropriate tabular format so that traditional approaches to CBR can be applied. In the case of image datasets this involves the application of segmentation and registration techniques. This paper proposes the adoption of an alternative approach to image representation whereby salient images features are encapsulated using time series.

Referring back to the two issues identified above the questions to be addressed are: (i) how can images best be translated into time series; and (ii) given an example time series represented image, how can we identify the most similar image within a Case Base (CB). With respect to the time series representation of images, we may consider images in their entirety or in terms of some sub region that features across the image set. The first takes into account the entire image while the second is directed at some specific feature within the image. Which is the most appropriate depends in part on the nature of the application. If the content of the entire image is important or if there is no single defining feature, then the first should be adopted. The second approach is only applicable if there is some feature that exists across the image set that is significant with respect to a particular application. Once a time series representation has been generated a similarity checking mechanism is required. Essentially this entails some form of *curve comparison*. The technique promoted in this paper is Dynamic Time Warping (DTW). This was selected because it is well understood and operates on curves that are not necessarily of the same unit length.

The intention of the paper is to provide an insight into the operation of time series analysis CBR with respect to the above. To act as a focus for the analysis, two specific applications are considered: (i) the screening of retinal images for Age-related Macular Degeneration (AMD), and (ii) the categorisation of Magnetic Resonance Imaging (MRI) brain scans. AMD is an eye condition that affects the macula, the central portion of the retina. It is the leading cause of irreversible blindness in the elderly and is a growing global healthcare challenge due to our ageing population; early detection may offer an opportunity for the application of timely treatment to inhibit the progress of the condition. A good way of identifying the early onset of AMD is through the identification of “fatty deposits” (called *drusen*) and pigment abnormality in the retina. Currently this is achieved by visual inspection, by clinicians, of the “fundus” photograph. This is a time consuming process and subject to human factors such as skills and tiredness; automated screening is therefore seen as beneficial even if only a coarse grading can be achieved.

The screening of retinal images for AMD requires the entire image to be taken into consideration. The second application, the categorisation of MRI brain scans is directed at a particular region within such scans, namely the *corpus callosum*. The corpus callosum connects the two hemispheres of the brain. It

is conjectured that the size and shape of the corpus callosum dictates certain human abilities (such as mathematical or musical abilities), human characterises (such as “handedness”) and certain medical conditions (such as epilepsy).

The rest of this paper is organised as follows. Section 2 provides some background with respect to time series analysis, DTW and CBR. The two applications, that form the focus of the work reported in this paper, are then described in Sections 3 and 4 respectively. The sections also include a full evaluation of the proposed approaches using real data. A summary and some conclusions are then presented in Section 5.

2 Background

Time Series Analysis (TSA) is concerned with the study of data that can be represented as one or more curves with a view to extracting knowledge using this representation. Note that the data dimensions do not necessarily need to include time, TSA may be applied to any form of data that can be represented as a sequence of one or more curves. The fundamental issues of TSA are: (i) how to measure similarity between time series and (ii) how to compress the time series while maintaining discriminatory power. Similarity can be measured in terms of ([2]): (i) similarity in time, (ii) similarity in shape and (iii) similarity in change. Related areas are Time Series Data Mining (TSDM), forecasting and the analysis of moving object data. An example of the last can be found in [24]. Keogh and Kasetty [18] give a survey of TSDM. For a discussion of time series forecasting see [1].

Dynamic Time Warping (DTW) is a technique whereby two time series can be compared. The technique does not require the two curves to be of the same length and takes into account a certain amount of “skew” to obtain a best fit. DTW was first proposed by Sakoe and Chiba [27] and was originally applied to speech recognition problems, but subsequently has been applied in much wider areas of application [19]. Given two time series: $Q = \{q_1, q_2, \dots, q_i, \dots, q_n\}$ and $C = \{c_1, c_2, \dots, c_j, \dots, c_m\}$, these can be aligned using DTW by constructing a n by m grid (matrix) such that the value for element (i, j) is the *squared Euclidean distance* from point c_j on curve C , a comparator sequence, to point q_i on curve Q , the query sequence, i.e. a sequence we wish to compare to C with the aim (say) of categorising Q . The best match between the two sequences Q and C is the *warping path* that minimises the total cumulative distance from grid element $(0, 0)$ to (n, m) . A warping path is any contiguous set of matrix elements from $(0, 0)$ to (n, m) . The warping cost associated with a particular path is its cumulative distance. DTW tends to produce better results than using a straight forward point-to-point comparison, however it tends to be computationally expensive. A number of tricks can be used to speed up the process. For example we can coarsen the data to produce an approximate path (i.e. do not use every sample point). Alternatively, from the observation that we can expect the best path to approximate to the line from $(0, 0)$ to (n, m) , we can omit many calculations. Work has been done on the nature of the *warping window* (for example use of the “Sakoe-Chiba band” or the “Itakura parallelogram”).

Case Based Reasoning (CBR) has a well established body of literature associated with it. Recommended reference works include [21] and [20]. For a review of the application of CBR in medical domains see [16] or [3]. For a discussion on the crossover between data mining and CBR interested readers are referred to [25].

3 AMD Screening

The motivation for AMD screening was introduced in Section 1. The objective is to detect the presence of drusen (a primary indicator of AMD) in retina images collected as part of a screening programme; thus we wish to categorise/classify retina images as positive (evidence of AMD detected) or negative (normal). Three example images are presented in Fig. 1. The image on the right (Fig. 1[c]) is from a normal eye, while the other two (Figures 1[a] and [b]) are images of eyes that contain drusen (light coloured flecks scattered across the image) and other pathological features. Inspection of the images indicates the difficulty in detecting the drusen. This is thus one of our motivations for employing CBR techniques, rather than to attempt to detect these features using other techniques such as image segmentation. The optic disc (OD), a bright coloured disc featured in the retinal images in Fig. 1 from which all blood vessels emanate, connects the retina to the “optic nerve”. The macula, clearly visible in the center of the image given in Fig. 1[c] as a dark coloured region, acts as a light detector and provides humans with the central vision essential for seeing fine details and with the colour vision (the macula is obscured by drusen in Figures 1[a] and [b]).

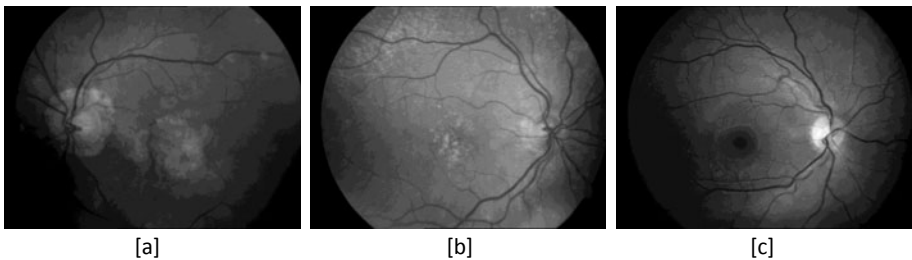


Fig. 1. Example of Retinal Images, [a] and [b] feature AMD, while [c] does not

3.1 Time Series CBR for AMD Screening

To represent images of the form shown in Fig. 1 the approach advocated in this paper is to consider the images in terms of pixel values using the Red-Green-Blue (RGB) colour model and the Hue-Saturation-Intensity (HSI) representation of the RGB model. As such each image can be represented as a sequence of histograms, with length M , to which a curve can easily be fitted. Each histogram is represented as a curve h_i , such that each point along the curve, $h_i(m)$ takes some value β (where $0 \leq m < M$, and β is the number of occurrences of intensity value m in image i).

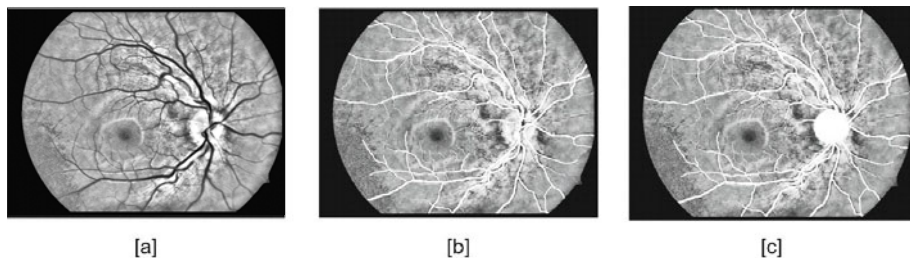


Fig. 2. Retinal images after [a] enhancement, [b] blood vessels removed and [c] optic disc removed

Prior to translating the images into time series some enhancement to the histograms was undertaken. The enhancement was done by applying a Contrast Limited Adaptive Histogram Equalisation (CLAHE) [33] technique. CLAHE computes histogram for different parts of an image and equalises each histogram separately. This image enhancement process increased the visibility of edges in the retinal images, as can be seen by comparing the enhanced image given in Fig. 2[a] with the image given in Fig. 1[c]. Initial experiments [13], indicated that the green and saturation channels produced the best results. The green channel was thus selected as the most appropriate for retina representation using the RGB model because of its ability to show the greatest contrast compared to other colour channels, seen as essential for retinal object identification [4,32]. The saturation component was selected as this has also been shown to produce good performance in identifying AMD featured retinal images [13]. The technique described here thus considers only the green and saturation channels. The length of the histograms, M , was set to 256 (number of RGB colour space cells) for the green channel histograms and 101 (with values ranging from 0 to 100) for the saturation histograms.

It was also found that the removal of pixels representing blood vessels enhanced the categorisation process. This was achieved by applying a retinal blood vessels segmentation algorithm [29] to segment the blood vessels. The identified blood vessels pixels were replaced by null values and consequently omitted from the histogram generation process. Fig. 2[b] gives an example of a retinal image with blood vessel pixels removed (indicated in white) by applying this process to the image given in Fig. 2[a].

Further experiments [14], indicated that the optic disc can obscure the presence of drusen. It is technically possible to remove the pixels representing the optic disc in the same way that blood vessel pixels were removed. To achieve this, a variation of optic disc detection using the horizontal and vertical axis of retinal images as proposed in [23] was applied. The retinal blood vessels binary image and the enhanced green channel image was utilised to generate both the horizontal and vertical signals, instead of using the original green channel image [23]. The optic disc pixel values were then replaced with null values.

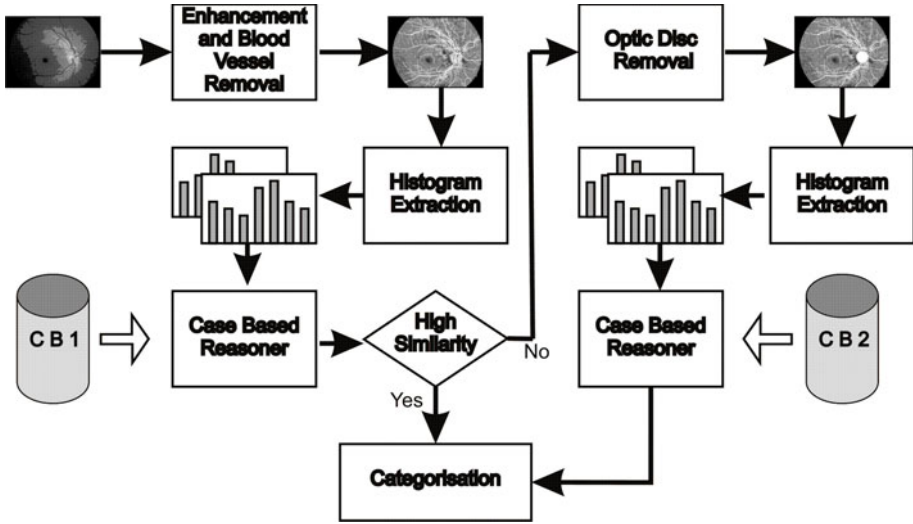


Fig. 3. Retina Image Categorisation Using Time Series CBR

Fig. 2[c] shows the retinal image given in Fig. 2[b] with the optic disc removed. It is also worth noting that the back coloured pixels (around the retina image) were excluded as well when the histograms were generated.

However, the routine removal of the optic disc can result in the removal of pixels representing drusen; especially where the drusen are close to, or superimposed over it. A two stage CBR approach is thus proposed consisting of two Case Bases (CBs), the primary CB and a secondary CB. The primary CB comprised the green and saturation histograms of labelled retina images (positive and negative) that included the optic disc but with blood vessels pixels removed, and the secondary CB comprised similar histograms but with the optic disc removed also.

A block diagram indicating the proposed CBR process is presented in Fig. 3. Given a new image we attempt to categorise this with reference to the primary CB first (CB1 in Fig. 3). The green channel histogram of the new image is compared to each of the green channel histograms in CB1 by means of computing the similarity measure between two histograms using DTW. A similar approach is also applied to the saturation histograms. These processes will generate the *preliminary results* comprising distance values between the green and saturation histograms of the new image, with the green and saturation histograms of each image in CB1. The *similarity* between the new image and each case in CB1 is then calculated by taking the average of each case's green and saturation histogram similarity values. If there exists only one "most similar" case, or there exist a number of most similar cases but all with the same label, the preliminary results will be taken as the final categorisation result and consequently the new image will be labelled as AMD or normal according to the label of the most similar image in CB1. If no clear result is obtained (i.e. there are two or more most similar cases with contradicting labels) the pixels representing the optic disc in

the new image are removed and the CBR process is repeated but this time with the secondary CB (CB2 in Fig. 3). For a more complete description interested readers are referred to [14].

3.2 AMD Screening Evaluation

To evaluate the time series CBR approach as applied to retina image screening a data set comprising 161 images, of which 101 were AMD featured images, were utilised. All of the images were acquired as part of ARIA¹ project, which aims to provide a platform that is capable of predicting eye disease risk on individuals at the point of image acquisition process.

Table 1. Results from AMD Screening Experiments

TCV run	Specificity (%)		Sensitivity (%)		Accuracy (%)	
	<i>CBs</i>	<i>SH</i>	<i>CBs</i>	<i>SH</i>	<i>CBs</i>	<i>SH</i>
1	67	67	82	91	77	82
2	50	33	60	80	56	63
3	84	83	100	90	94	88
4	84	67	90	80	88	75
5	67	50	100	90	88	75
6	83	50	80	70	81	63
7	50	67	90	100	75	88
8	67	50	90	90	81	75
9	67	33	70	70	69	56
10	67	33	100	100	88	75
Average	68	56	86	86	80	74

The results of the evaluation, using Ten-fold Cross Validation (TCV) are given in Table 1. The table gives values for the *specificity*, *sensitivity*, and *accuracy* recorded for each TCV. Results obtain using the above approach (columns marked CBs) were compared with results obtained using a spatial-histogram approach [15]. From the table it can be seen that the proposed approach, that is advocated in this paper, provides the best results with 80% accuracy, and an average increase of 5% over all evaluation metrics.

4 MRI Scan Categorisation

The second application considered in this paper is the categorisation of MRI brain scans according to a single feature within those scans, namely the corpus callosum. The objective of the study was to investigate the application of time series CBR in the context of a Region of Interest (ROI) contextualisation. As noted in Section 1 the study of the nature (shape and size) of the corpus callosum in MRI brain scans is of interest to the medical community with respect to

¹ [http://www.eyecharity.com/aria\\$_online/](http://www.eyecharity.com/aria$_online/)

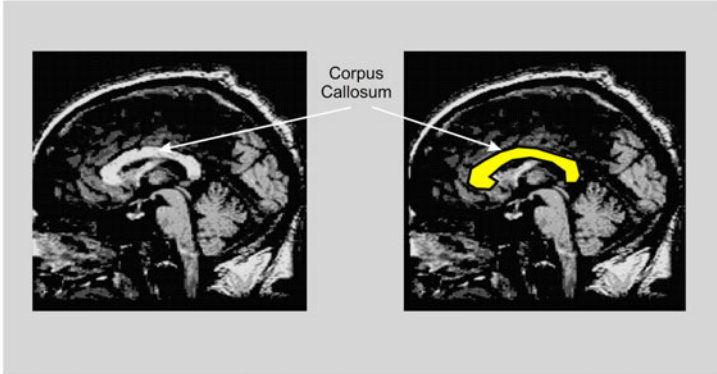


Fig. 4. Midsagittal MRI brain scan slice showing the corpus callosum (highlighted in the right-hand image)

certain medical conditions that affect the function of the brain and particular skills. The size and shape of the corpus callosum has been shown to be correlated to gender, age, neurodegenerative diseases and various lateralised behaviour in people such as “handedness”. It is also conjectured that the size and shape of the corpus callosum reflects certain human characteristics (such as a mathematical or musical ability). Several studies indicate that the size and shape of the corpus callosum, in humans, is correlated to gender [7,28], age [28,31], brain growth and degeneration [12,22], handedness [6], epilepsy [5,26,30] and brain dysfunction [8,17].

Fig. 4 gives an example (midsagittal slice) of a MRI brain scan. The corpus callosum is located at the center of the image (highlighted in the image on the right). Fig. 4 also highlights a related structure called the fornix the significance of which is that image segmentation techniques frequently find it difficult to determine where the corpus callosum ends and the fornix starts. The focus of the study described here is directed at the categorising of MRI brain scan images according to corpus callosum, but could equally be applied to the characterisation of other types of image that feature a given object.

4.1 Time Series CBR for MRI Scan Categorisation

When attempting to categorise images according to the nature of a particular feature, regardless of whether a CBR technique or some other techniques is to be used, the first issue is to identify and isolate the feature of interest. In the case of the corpus callosum we know, approximately, where it is located with respect to the boundaries of an MRI brain scan. Thus we can apply a segmentation algorithm to identify the corpus callosum pixels. For the work described here the *efficient graph-based segmentation* algorithm [11] was used. This method is based on Minimum Spanning Trees (MST). All pixels of the original image are viewed

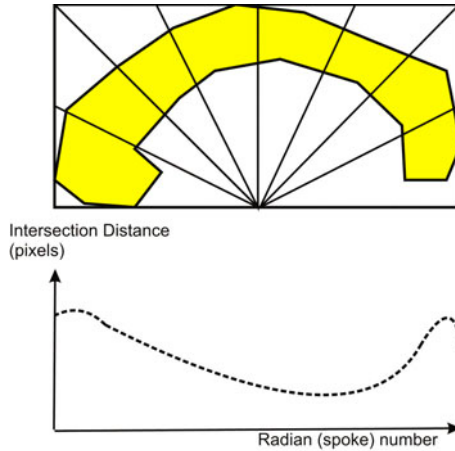


Fig. 5. Corpus callosum time series generation

as separate components. Two components are merged if the external variation between the components is small compared to the internal variation. Note that the segmentation can be problematic as a related tissue structure, the Fornix (also shown in the example given in Fig. 4) is often included together with some other spurious pixel clusters. Some data cleaning must therefore be undertaken. A smoothing technique was first applied to the MRI scans before the application of segmentation so as to preserve the boundaries between regions. This smoothing operation had the overall effect of bringing points in a cluster closer together.

Once the corpus callosum was identified we wish to represent it as a time series so that our proposed time series CBR technique could be applied. The adopted time series generation approach is illustrated in Fig. 5. A series of “spokes” were radiated out from the mid-point of the base of the Minimum Bounding Rectangle (MBR) surrounding a detected corpus callosum. The interval between spokes was one pixel measured along the edge of the MBR. Consequently, the number of spokes used to encode a corpus callosum varied from image to image. For each spoke the distance D_i (where i is the spoke identification number) over which the spoke intersects with a sequence of corpus callosum pixels was recorded. The mid point along the base of the MBR was chosen as this would ensure that there was only one intersection per spoke. The result is a time series with the spoke number i representing time and the value D_i , for each spoke, the magnitude. By plotting the D_i against i a time series may be derived (as shown in Fig. 5).

To categorise “unseen” MRI brain scans, according to the nature of the corpus callosum, an appropriate Case Base (CB) was constructed comprising labelled curves generated in the manner described above. A new case could then be compared, using DTW, to identify the most similar curve(s) in the CB. Further information on the categorisation of MRI brain scans according to the nature of the corpus callosum can be found in [9] and [10].

4.2 MRI Categorisation Evaluation

This section describes the evaluation of the proposed technique using “real life” MRI image sets. The evaluation was undertaken in terms of classification accuracy, sensitivity and specificity. Three studies are reported here: (i) a comparison between musician and non-musician MRI scans, (ii) a comparison between MRI scans belonging to right handed and left handed people, and (iii) an epilepsy screening process. The studies are discussed in more detail below.

Musicians v. Non-Musicians. For the musicians study a data set comprising 106 MRI scans was used, 53 representing musicians and 53 non-musicians, the data set was thus divided into two equal classes. The study was of interest because of the conjecture that the size and shape of the corpus callosum reflects certain human abilities (such as a mathematical or musical ability). Table 2 shows the TCV results obtained using the proposed technique. Inspection of Table 2 demonstrates that the overall classification accuracy of the time series CBR approach is significantly high. In many TCV cases the time series based approach obtained 100% accuracy, even though visual inspection of the corpus callosums in the image set does not lead to any clear identification of any defining feature.

Table 2. TCV Classification Results from Musicians Study

Test set ID	Accuracy(%)	Sensitivity(%)	Specificity (%)
1	91	100	85.71
2	100	100	100
3	91	100	85.71
4	100	100	100
5	100	100	100
6	100	100	100
7	100	100	100
8	100	100	100
9	100	100	100
10	100	100	100
Average	98.2	100	97.14
SD	3.8	0.0	6.03

Right handed v. Left handed. For the handedness study a data set comprising 82 MRI scans was used, 42 representing right handed people and 40 left handed people. The study was of interest because of the conjecture that the size and shape of the corpus callosum reflects certain human characteristics (such as handedness). Table 3 shows the TCV results obtained using the proposed technique. Inspection of Table 2 demonstrates that the overall classification accuracy of the time series CBR approach was again significantly high.

Epilepsy Screening. For the epilepsy study three datasets were used:

1. The first comprised the control group from the above musicians study together with 53 MRI scans from epilepsy patients.
2. The second data set used all 106 MRI scans from the musicians study as the control group, and the 53 epilepsy scans.
3. The third comprised all 106 MRI scans from the musicians study and a further 106 epilepsy cases so that the control and epilepsy groups were of equal size.

The aim of the study was to seek support for the conjecture that the shape and size of the corpus callosum is influenced by conditions such as epilepsy ([26,30]). Table 4 shows the TCV classification results for the three epilepsy data sets. Inspection of Table 4 indicates that the time series CBR approach performed significantly well in the context of distinguishing epilepsy MRI scans from the control group.

Table 3. TCV Classification Results from Handedness Study

Test set ID	Accuracy(%)	Sensitivity(%)	Specificity (%)
1	88.89	80	100
2	100	100	100
3	100	100	100
4	88.89	100	80
5	88.89	75.0	100
6	100	100	100
7	100	100	100
8	100	100	100
9	100	100	100
10	100	100	100
Average	96.67	95.5	98
SD	5.37	9.56	6.32

Table 4. TCV Classification Results for Epilepsy Study

Test set ID	106 MR scans			159 MR scans			212 MR scans		
	Acc.	Sens.	Spec.	Acc.	Sens.	Spec.	Acc.	Sens.	Spec.
1	72.73	80.00	66.67	75.00	70.00	83.33	81.82	88.89	76.92
2	81.82	83.33	80.00	81.25	85.71	77.78	77.27	80.00	75.00
3	72.73	80.00	66.67	75.00	70.00	83.33	81.82	88.89	76.92
4	81.82	83.33	80.00	81.25	85.71	77.78	77.27	80.00	75.00
5	81.82	83.33	80.00	81.25	85.71	77.78	68.18	70.00	66.67
6	81.82	83.33	80.00	75.00	70.00	83.33	72.73	77.78	69.23
7	63.64	66.67	60.00	81.25	85.71	77.78	77.27	80.00	75.00
8	81.82	83.33	80.00	68.75	66.67	71.43	81.82	88.89	76.92
9	72.73	80.00	66.67	68.75	66.67	71.43	72.73	77.78	69.23
10	63.64	66.67	60.00	81.25	85.71	77.78	81.82	88.89	76.92
Average	75.46	79.0	72.0	76.88	77.19	78.18	77.27	82.11	73.78
SD	7.48	6.67	8.78	5.15	9.06	4.37	4.79	6.51	3.89

4.3 Discussion of Results

With respect to classification accuracy the time series CBR approach performed well. Although the time series approach produced good results there was no obvious reason why this might be the case; visual inspection of the MRI scans did not indicate any obvious distinguishing attributes with respect to the size and shape of the corpus callosum. Further investigation is therefore deemed to be appropriate. With respect to computational complexity, image segmentation and the application of DTW for categorisation of images are both computationally expensive processes. The time complexity for the image segmentation was about 30 seconds per image. For the given data sets the application of DTW required, on average, 90 seconds to complete the classification of the entire test set.

5 Summary and Conclusion

In this paper an approach to the categorisation of images using a time series based CBR approach has been described. Two variations of the approach were considered. An investigation of its application using entire images, and an investigation of its application with respect to a specific region of interest in common across a set of images. The first was illustrated using an AMD screening programme applied to retina images. The second was demonstrated by considering the categorisation of MRI brain scans according to a particular feature common across such images, namely the corpus callosum. Both techniques used the “tried and tested” technique of Dynamic Time Warping to comparing images contained in a case base with a new image to be categorised. Different time series generation processes were demonstrated, and although these were specific to the applications under consideration it is argued that they have general utility. Evaluation of the approach, using “real life” data produced excellent results. Best results were produced in the context of the MRI brain scan data, although the reason for these excellent results requires further investigation.

References

1. Aburto, L., Weber, R.: A Sequential Hybrid Forecasting System for Demand Prediction. In: Perner, P. (ed.) *MLDM 2007*. LNCS (LNAI), vol. 4571, pp. 518–532. Springer, Heidelberg (2007)
2. Bagnall, A., Janacek, G.: Clustering Time Series with Clipped Data. *Machine Learning* 58, 151–178 (2005)
3. Bichindaritz, I., Marling, C.: Case-based reasoning in the health sciences: What’s next? *Artificial Intelligence in Medicine* 36(2), 127–135 (2006)
4. Chaudhuri, S., Chatterjee, S., Katz, N., Nelson, M., Goldbaum, M.: Detection of Blood Vessels in Retinal Images using Two-Dimensional Matched Filters. *IEEE Transactions on Medical Imaging* 8(3), 263–269 (1989)
5. Conlon, P., Trimble, M.: A Study of the Corpus Callosum in Epilepsy using Magnetic Resonance Imaging. *Epilepsy Res.* 2, 122–126 (1988)
6. Cowell, P., Kertesz, A., Denenberg, V.: Multiple Dimensions of Handedness and the Human Corpus Callosum. *Neurology* 43, 2353–2357 (1993)

7. Davatzikos, C., Vaillant, M., Resnick, S., Prince, J., Letovsky, S., Bryan, R.: A Computerized Approach for Morphological Analysis of the Corpus Callosum. *Journal of Computer Assisted Tomography* 20, 88–97 (1996)
8. Duara, R., Kushch, A., Gross-Glenn, K., Barker, W., Jallad, B., Pascal, S., Loewenstein, D., Sheldon, J., Rabin, M., Levin, B., Lubs, H.: Neuroanatomic Differences Between Dyslexic and Normal Readers on Magnetic resonance Imaging Scans. *Archives of Neurology* 48, 410–416 (1991)
9. Elsayed, A., Coenen, F., Jiang, C., García-Fiñana, M., Sluming, V.: Region Of Interest Based Image Classification Using Time Series Analysis. In: *IEEE International Joint Conference on Neural Networks*, pp. 3465–3470 (2010)
10. Elsayed, A., Coenen, F., Jiang, C., García-Fiñana, M., Sluming, V.: Corpus Callosum MR Image Classification. *Knowledge Based Systems* 23(4), 330–336 (2010)
11. Felzenszwalb, P., Huttenlocher, D.: Efficient Graph-based Image Segmentation. *Int. Journal of Computer Vision* 59(2), 167–181 (2004)
12. Hampel, H., Teipel, S., Alexander, G., Horwitz, B., Teichberg, D., Schapiro, M., Rapoport, S.: Corpus Callosum Atrophy is a Possible Indicator of Region and Cell Type-Specific Neuronal Degeneration in Alzheimer Disease. *Archives of Neurology* 55, 193–198 (1998)
13. Hijazi, M.H.A., Coenen, F., Zheng, Y.: A Histogram Based Approach to Screening of Age-related Macular Degeneration. In: *Proc. of Medical Image Understanding and Analysis (MIUA 2009)*, pp. 154–158 (2009)
14. Hijazi, M.H.A., Coenen, F., Zheng, Y.: Retinal Image Classification using a Histogram Based Approach. In: *IEEE International Joint Conference on Neural Networks*, pp. 3501–3507 (2010)
15. Hijazi, M.H.A., Coenen, F., Zheng, Y.: Retinal Image Classification for the Screening of Age-related Macular Degeneration. In: *Proceedings of SGAI Conference*, pp. 325–338 (2010)
16. Holt, A., Bichindaritz, I., Schmidt, R., Perner, P.: Medical Applications in Case-Based Reasoning. *The Knowledge Engineering Review* 20, 289–292 (2005)
17. Hynd, G., Hall, J., Novey, E., Eliopoulos, D., Black, K., Gonzalez, J., Edmonds, J., Riccio, C., Cohen, M.: Dyslexia and Corpus Callosum Morphology. *Archives of Neurology* 52, 32–38 (1995)
18. Keogh, E., Kasetty, S.: On the Need for Time Series Data Mining Benchmarks: A Survey and Empirical Demonstration. *Data Mining and Knowledge Discovery* 7(4), 349–371 (2003)
19. Keogh, E., Pazzani, M.: Scaling up dynamic time warping to massive datasets. In: Żytkow, J.M., Rauch, J. (eds.) *PKDD 1999. LNCS (LNAI)*, vol. 1704, pp. 1–11. Springer, Heidelberg (1999)
20. Kolodner, J.L.: *Case-based Reasoning*. Morgan Kaufmann Series in Representation and Reasoning (1993)
21. Leake, D.B.: *Case-based Reasoning: Experiences, Lessons and Future Directions*. AAAI Press Co-Publications (1996)
22. Lyoo, I., Satlin, A., Lee, C.K., Renshaw, P.: Regional Atrophy of the Corpus Callosum in Subjects with Alzheimer’s Disease and Multi-infarct Dementia. *Psychiatry Research* 74, 63–72 (1997)
23. Mahfouz, A.E., Fahmy, A.S.: Ultrafast Localization of the Optic Disc using Dimensionality Reduction of the Search Space. In: *Medical Image Computing and Computer Assisted Intervention*, pp. 985–992 (2009)
24. Morzy, M.: Mining Frequent Trajectories of Moving Objects for Location Prediction. In: Perner, P. (ed.) *MLDM 2007. LNCS (LNAI)*, vol. 4571, pp. 667–680. Springer, Heidelberg (2007)

25. Pal, S., Aha, D., Gupta, K.: *Case-Based Reasoning in Knowledge Discovery and Data Mining*. Wiley-Blackwell (in Press, 2011)
26. Riley, J.D., Franklin, D.L., Choi, V., Kim, R.C., Binder, D.K., Cramer, S.C., Lin, J.J.: Altered White Matter Integrity in Temporal Lobe Epilepsy: Association with Cognitive and Clinical Profiles. *Epilepsia* 42(4), 536–545 (2010)
27. Sakoe, H., Chiba, S.: Dynamic Programming Algorithm Optimization for Spoken Word Recognition. *IEEE Transactions on Acoustics, Speech and Signal Processing* 26(1), 43–49 (1978)
28. Salat, D., Ward, A., Kaye, J., Janowsky, J.: Sex Differences in the Corpus Callosum with Aging. *Journal of Neurobiology of Aging* 18, 191–197 (1997)
29. Soares, J.V.B., Leandro, J.J.G., Cesar Jr., R.M., Jelinek, H.F., Cree, M.J.: Retinal Vessel Segmentation using the 2-D Gabor Wavelet and Supervised Classification. *IEEE Transactions on Medical Imaging* 25, 1214–1222 (2006)
30. Weber, B., Luders, E., Faber, J., Richter, S., Quesada, C.M., Urbach, H., Thompson, P.M., Toga, A.W., Elger, C.E., Helmstaedter, C.: Distinct Regional Atrophy in the Corpus Callosum of Patients with temporal Lobe Epilepsy. *Brain* 130, 3149–3154 (2007)
31. Weis, S., Kimbacher, M., Wenger, E., Neuhold, A.: Morphometric Analysis of the Corpus Callosum using MRI: Correlation of Measurements with Aging in Healthy Individuals. *American Journal of Neuroradiology* 14, 637–645 (1993)
32. Youssif, A.A.-H., Ghalwash, A.Z., Ghoneim, A.A.A.-R.: Optic Disc Detection from Normalized Digital Fundus Images by Means of A Vessel's Direction matched Filter. *IEEE Transactions on Medical Imaging* 27, 11–18 (2008)
33. Zuiderveld, K.: Contrast Limited Adaptive Histogram Equalization. *Academic Press Graphics Gems Series*, pp. 474–485 (2001)